

Article

Not peer-reviewed version

Local Feynman Diagrammatics in Curved Spacetime: A Consistent LMC Framework

[Fridolin Weber](#)*

Posted Date: 26 February 2026

doi: 10.20944/preprints202602.1722.v1

Keywords: quantum field theory in curved spacetime; Local Minkowski Coordinates (LMC); WKB approximation; curvature-dependent propagators; feynman diagrams in curved backgrounds; hawking radiation



Preprints.org is a free multidisciplinary platform providing preprint service that is dedicated to making early versions of research outputs permanently available and citable. Preprints posted at Preprints.org appear in Web of Science, Crossref, Google Scholar, Scilit, Europe PMC.

Copyright: This open access article is published under a [Creative Commons CC BY 4.0 license](#), which permit the free download, distribution, and reuse, provided that the author and preprint are cited in any reuse.

Disclaimer/Publisher's Note: The statements, opinions, and data contained in all publications are solely those of the individual author(s) and contributor(s) and not of MDPI and/or the editor(s). MDPI and/or the editor(s) disclaim responsibility for any injury to people or property resulting from any ideas, methods, instructions, or products referred to in the content.

Article

Local Feynman Diagrammatics in Curved Spacetime: A Consistent LMC Framework

Fridolin Weber^{1,2} 

¹ Department of Physics, San Diego State University (SDSU), San Diego, USA; fweber@sdsu.edu

² Department of Physics, University of California at San Diego (UCSD), La Jolla, USA

Abstract

We develop a general framework for quantum field theory in curved spacetime based on Local Minkowski Coordinates (LMC), which incorporates curvature effects into local Feynman diagrammatics. Gravitational influence enters through a curvature-dependent normalization function $B(x)$, derived from covariant current conservation, and a gravitational phase $S(x)$, obtained via the WKB approximation. These quantities enter through local phase accumulation and observer-dependent normalization of external states, without affecting global observables. As a first application, we analyze the local redshift normalization and phase structure of quantum amplitudes in the vicinity of a Schwarzschild black hole. Within their range of validity, the curvature-dependent factors $B(x)$ and $S(x)$ reproduce the expected gravitational redshift of field amplitudes in general relativity. When amplitudes are propagated to asymptotic infinity and evaluated in a standard global quantum state (such as the Unruh state), the resulting flux is consistent with the standard Hawking result. The framework refines the local WKB structure and clarifies the separation between local normalization effects and globally conserved fluxes.

Keywords: quantum field theory in curved spacetime; Local Minkowski Coordinates (LMC); WKB approximation; curvature-dependent propagators; feynman diagrams in curved backgrounds; hawking radiation

1. Introduction

Quantum field theory in curved spacetime (QFT-CS) extends the principles of ordinary quantum field theory to settings where classical gravitational fields influence quantum processes. In contrast to quantum gravity, which attempts to quantize the spacetime metric itself, QFT-CS treats the geometry as fixed and non-dynamical. This semiclassical framework has become a cornerstone of modern theoretical physics, providing essential insight into black-hole thermodynamics, cosmological particle creation, and early-universe dynamics.

It underlies several central results at the interface of quantum mechanics and general relativity, including Hawking radiation [1], cosmological particle production in expanding universes [2,3], and the Unruh effect [4]. All of these arise from quantum field theory in nontrivial backgrounds, including curved geometries and observer-dependent notions of particles. Despite its success, much of the standard formalism relies on global mode decompositions and the assumption of preferred vacuum states, assumptions that can fail in generic or time-dependent spacetimes lacking global symmetries or Killing vectors.

Recent work on curvature-dependent amplitudes and local WKB constructions has blurred the distinction between local normalization effects and globally conserved fluxes, leading to claims of enhanced black-hole emission [5,6]. We develop a local diagrammatic framework that separates single-point normalization from bi-local geometric propagation and explains why the Hawking flux at asymptotic infinity remains unchanged when observables are evaluated in a standard quantum state.

To address these limitations, we employ the Local Minkowski Coordinates (LMC) approach, which leverages the equivalence principle to approximate small neighborhoods of curved spacetime as locally flat. In each convex normal neighborhood, fields are expanded in local inertial coordinates, allowing a patchwise construction of quantum amplitudes without the need for global mode bases or globally defined vacua. This framework naturally incorporates curvature effects through two geometric structures: a normalization function $B(x)$, derived from covariant current conservation, and a gravitational phase $S(x)$, determined from the Hamilton–Jacobi equation. Together they modify propagators and interaction vertices while leaving the topological structure of Feynman diagrams unchanged.

As a practical example, we apply the formalism to a Yukawa interaction in a weakly curved Schwarzschild background to illustrate how gravitational redshift modifies the local normalization and phase of quantum fields. These corrections are local in nature and vanish in the flat-spacetime limit. When observables are evaluated at asymptotic infinity within a chosen global quantum state (e.g. the Unruh state), the total flux and spectral shape are consistent with the standard Hawking result.

Throughout this paper, we adopt units where $c = 1$. The gravitational constant G is retained explicitly to keep track of dimensional quantities, particularly in expressions involving curvature scales and black hole parameters. Mass, energy, and inverse length are therefore interchangeable, and all curvature tensors have mass dimension two. When needed, we restore physical units for clarity, especially in the discussion of observational consequences. For derivatives, we distinguish between covariant and ordinary ones. The symbol ∇_μ denotes the covariant derivative associated with the background metric $g_{\mu\nu}$, while ∂_μ is reserved for ordinary derivatives in local inertial coordinates (Riemann normal coordinates) centered at x_0 , or for partial derivatives acting on scalars in a chosen chart. In particular, the conserved current takes the form

$$j^\mu = B^2(x) \partial^\mu S(x), \quad \nabla_\mu j^\mu = 0, \quad (1)$$

so that current conservation is always expressed with ∇_μ , not ∂_μ . This ensures consistency between the WKB transport equation and covariant flux conservation.

2. Local Minkowski Coordinates and Field Quantization

The starting point of our approach is the equivalence principle, which states that the laws of physics in a sufficiently small neighborhood of any spacetime point are indistinguishable from those of flat spacetime. This motivates the introduction of LMC, a system $\{\zeta^\mu\}$ in which the metric $g_{\mu\nu}(x)$ approximates the Minkowski metric $\eta_{\mu\nu}$ to leading order. In Riemann normal coordinates centered at a reference point x_0 , the metric expansion takes the form

$$g_{\mu\nu}(x) = \eta_{\mu\nu} - \frac{1}{3} R_{\mu\alpha\nu\beta}(x_0) \zeta^\alpha \zeta^\beta + \mathcal{O}(\zeta^3), \quad (2)$$

where the curvature tensor is evaluated at x_0 . In Riemann normal coordinates centered at x_0 , the local Minkowski patch shown in Figure 1 provides the geometric setting for this expansion. Each shaded region represents a local Minkowski patch, a convex normal neighborhood within which the metric is well approximated by Equation (2) and curvature effects are negligible. The dashed curves denote sample geodesics connecting adjacent patches, and the central arrows labeled ζ^0 and ζ^1 indicate the temporal and spatial axes of the local inertial frame centered at x_0 . Only the ζ^0 – ζ^1 plane of this local coordinate system is shown.

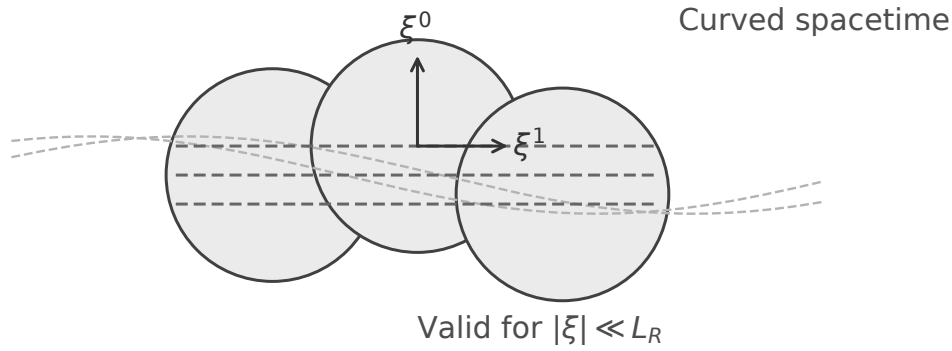


Figure 1. Schematic illustration of LMC patches in a curved spacetime. Three overlapping shaded disks represent convex normal neighborhoods in which the metric is locally flat and fields admit the WKB form of Equation (3). The dashed lines depict sample geodesics traversing the patches, while the central arrows labeled ξ^0 and ξ^1 indicate the local temporal and spatial axes of the inertial frame centered at x_0 . Only the ξ^0 – ξ^1 plane of this local frame is shown. The construction is valid for $|\xi| \ll L_R$ and breaks down near horizons where curvature gradients become large.

In this local frame, a scalar or fermionic field can be expressed using a WKB-inspired ansatz,

$$\Phi(x) \simeq B(t, x) e^{iS(t, x)/\hbar} \Phi_{\text{flat}}(\xi), \quad (3)$$

where $B(t, x)$ is a real amplitude encoding geometric redshift and $S(t, x)$ is a gravitational phase determined by the local geometry. The flat-space component $\Phi_{\text{flat}}(\xi)$ satisfies the standard Minkowski equation. Equation (3) holds within a convex normal neighborhood where geodesics do not intersect and curvature variations are small.

Two independent small parameters control this approximation: (i) a geometric locality condition $|\xi|/L_R \ll 1$, where $L_R \sim |R_{\mu\nu\rho\sigma}|^{-1/2}$ is the curvature scale, and (ii) the semiclassical hierarchy $|\partial B/B| \ll |\partial S|$, ensuring that the phase varies much more rapidly than the amplitude. When both conditions are satisfied, the LMC framework provides a consistent procedure for embedding flat-space Feynman diagrammatics into weakly curved backgrounds.

3. Normalization, Phase, and Validity of the Local Expansion

The functions $B(x)$ and $S(x)$ follow directly from the WKB expansion of the Klein–Gordon equation $(\square - m^2)\Phi = 0$. Substituting Equation (3) and expanding in powers of \hbar yields, to leading orders,

$$\mathcal{O}(\hbar^{-2}) : g^{\mu\nu} \partial_\mu S \partial_\nu S = m^2, \quad (4)$$

$$\mathcal{O}(\hbar^{-1}) : 2\nabla_\mu B \partial^\mu S + B \square S = 0, \quad (5)$$

Equations (4) and (5) represent the leading terms of the WKB hierarchy, corresponding respectively to the Hamilton–Jacobi and transport equations that determine the phase $S(x)$ and the amplitude $B(x)$.

At the bi-local level, short-distance geodesic focusing is encoded by the Van Vleck–Morette determinant

$$\Delta(x, x') = -g^{-1/2}(x) g^{-1/2}(x') \det[-\nabla_\mu \nabla_{\nu'} \sigma(x, x')], \quad (6)$$

where $\sigma(x, x')$ is Synge’s world function, equal to one-half the squared geodesic distance between x and x' . The dressed two-point function then has the universal Hadamard form

$$G_F(x, x') \sim \frac{\Delta^{1/2}(x, x')}{4\pi^2(\sigma + i\epsilon)} + \dots, \quad (7)$$

which preserves the correct short-distance behavior in curved spacetime. The single-point WKB factor $B(x)$ remains a local transport amplitude (governing external legs and local insertions) and is distinct

from the bi-local focusing factor $\Delta^{1/2}(x, x')$ that appears in G_F . In stationary-phase matching of vertex integrals, the Hessian determinant at the geodesic saddle combines with the local Jacobian $|\partial\xi/\partial x|$ to reproduce $\Delta^{1/2}(x, x')$, ensuring a unitary leading-order matching between patches.

For null propagation the transport equation reduces to $\nabla_\mu(B^2 k^\mu) = 0$ with $k^\mu = \nabla^\mu S$ the local wave vector, so that $B \propto \Delta^{1/2}$ along null geodesics. Hence even in the massless limit the amplitude varies with the expansion $\theta = \nabla_\mu k^\mu$ of the null congruence rather than remaining constant. The conserved current,

$$j^\mu = \frac{i}{2\hbar} (\Phi^* \nabla^\mu \Phi - \Phi \nabla^\mu \Phi^*) = B^2 \partial^\mu S, \quad (8)$$

satisfies $\nabla_\mu j^\mu = 0$, confirming that $B(x)$ acts as a local normalization ensuring covariant flux conservation along the classical flow defined by $S(x)$.

For a static metric with

$$ds^2 = -f(r)dt^2 + f^{-1}(r)dr^2, \quad (9)$$

inserting

$$S = \omega t - \int dr (\omega/f) \quad (10)$$

into Equation (5) gives

$$B \propto f^{-1/4} = (-g_{00})^{-1/4}. \quad (11)$$

Equation (11) represents the redshift normalization factor associated with the time–radial sector of the metric and the choice of static observers. In a full four-dimensional Schwarzschild spacetime, additional geometric effects such as angular spreading of wavefronts and greybody transmission factors further influence the amplitude of radiative modes. These global and geometric effects are not captured by the local normalization factor $B(r)$ and are treated separately in standard analyses. In the present framework, $B(r)$ should therefore be interpreted strictly as the local redshift normalization entering the WKB transport equation, rather than as the complete radial dependence of physical fluxes. It represents a local normalization factor rather than a global enhancement of radiative power or particle number. When integrated over a complete hypersurface, the conserved flux derived from j^μ remains invariant, ensuring consistency with global energy conservation.

The LMC framework relies on the assumption that curvature effects can be treated perturbatively inside each local patch. The expansion in Equation (2) is valid as long as

$$|\xi|^2 \ll \frac{1}{|R_{\alpha\beta\gamma\delta}(x_0)|}, \quad (12)$$

so that higher-order terms involving curvature derivatives remain negligible.

To quantify the range of validity, it is convenient to introduce dimensionless expansion parameters

$$\epsilon_{\text{curv}} = \frac{\ell_{\text{wave}}}{L_R}, \quad \epsilon_{\text{grad}} = \frac{\ell_{\text{wave}}}{L_{\nabla R}}, \quad \epsilon_{\text{int}} = \lambda \ell_{\text{wave}}^2 E^2, \quad (13)$$

where $\ell_{\text{wave}} \sim E^{-1}$ is the typical wavelength, $L_R \sim |R_{\mu\nu\rho\sigma}|^{-1/2}$ the curvature radius, and $L_{\nabla R} \sim |\nabla R_{\mu\nu\rho\sigma}|^{-1/3}$ the scale of curvature variation. The LMC expansion is reliable provided $\epsilon_{\text{curv}}, \epsilon_{\text{grad}}, \epsilon_{\text{int}} \ll 1$. For a $10 M_\odot$ black hole, using $L_R \sim |R|^{-1/2}$ with $|R| = \sqrt{48} GM/r^3$, one finds $L_R \approx 2.9 \times 10^4$ m at $r = 3GM$, implying $\epsilon_{\text{curv}} \sim 7 \times 10^{-21}$ for GeV scale quanta. For Schwarzschild, the Kretschmann scalar is $K \equiv R_{\mu\nu\rho\sigma} R^{\mu\nu\rho\sigma} = 48 G^2 M^2 / r^6$. With our norm $|R| \equiv \sqrt{K}$, the curvature radius is

$$L_R \sim |R|^{-1/2} = \frac{r^{3/2}}{48^{1/4} \sqrt{GM}}. \quad (14)$$

At $r = 6GM$ and $M = 10 M_\odot$, using Equation (14) to evaluate the curvature radius L_R , one finds $L_R \approx 8.2 \times 10^4$ m (≈ 82 km). The Hawking temperature corresponds to the angular frequency $\omega_H =$

$k_B T_H / \hbar = c^3 / (8\pi GM)$.¹ Numerically $\omega_H \approx 8.1 \times 10^2 \text{ s}^{-1}$ for $10 M_\odot$, so the reduced wavelength is $\ell_{\text{wave}} \sim c / \omega_H \approx 3.7 \times 10^5 \text{ m}$. Hence

$$\epsilon_{\text{curv}} = \frac{\ell_{\text{wave}}}{L_R} \approx \frac{3.7 \times 10^5 \text{ m}}{8.2 \times 10^4 \text{ m}} \approx 4.5 \quad (r = 6GM, \omega \sim \omega_H), \quad (15)$$

indicating that the geometric-optics/WKB expansion is *not* yet parametrically small for quanta at the thermal peak so deep in the potential. For higher energies or farther out the expansion improves rapidly: at $r = 10GM$ one has $L_R \simeq 1.77 \times 10^5 \text{ m}$, giving $\epsilon_{\text{curv}} \approx 0.21$ for $\omega = 10 \omega_H$ (and ≈ 0.11 for $\omega = 20 \omega_H$). These estimates quantify where the LMC/WKB treatment is accurate: either for quanta with $\omega \gg \omega_H$ or at radii where L_R is larger (weaker curvature), consistent with the conditions in Equations (14) to (17).

In what follows we require a quantitative small parameter:

$$\epsilon(x) \equiv \frac{\lambda_{\text{ph}}(x)}{L_{\text{curv}}(x)} \lesssim 0.3, \quad (16)$$

so that subleading transport/Hadamard terms remain controlled. Accordingly, all statements and plots are restricted to radii/frequencies satisfying Equation (16). Near $r \approx 6GM$ at $\omega \sim \omega_H$ the expansion is not parametrically small and results are qualitative only.

In black-hole spacetimes, Equation (11) formally diverges as $g_{00} \rightarrow 0$, signaling the breakdown of the local expansion rather than a physical infinity. The method should therefore be restricted to regions satisfying

$$\ell_{\text{patch}} \ll L_R, \quad (17)$$

where ℓ_{patch} denotes the characteristic size of the local Riemann-normal neighborhood. Otherwise geodesic convergence and strong-field effects invalidate the Riemann normal coordinate expansion. Outside convex normal neighborhoods, multiple geodesics or conjugate points can occur and $\Delta^{1/2}(x, x')$ may vanish. In such regions the present leading-order LMC description must be patched across saddles (including the appropriate Maslov phases) or replaced by a full Hadamard expansion.

Condition (17) should be understood as a geometric requirement ensuring that the local Riemann-normal expansion remains valid within a convex normal neighborhood and that geodesic focusing does not invalidate the WKB hierarchy. In practice, the operative control parameters of the LMC expansion are the local smallness conditions $|\zeta| \ll L_R$ and $\epsilon \equiv \lambda_{\text{ph}} / L_{\text{curv}} \ll 1$, as defined in Equation (16). For sufficiently high-frequency modes, these conditions may remain satisfied closer to the horizon, while for modes near the Hawking scale the breakdown occurs earlier. All results presented here are restricted to regions where these local control parameters remain small.

The radial behavior of the local normalization function $B(r)$, together with the Tolman redshift factor $(-g_{00})^{-1/2}$, is shown in Figure 2. Both functions increase sharply as $r \rightarrow 2GM$, reflecting the gravitational redshift of static coordinates in the static frame. The divergence is not physical but marks the limit of applicability of the WKB and Riemann-normal expansions. Beyond this region, the local LMC approximation fails.

¹ Here, the speed of light c is restored for numerical estimates.

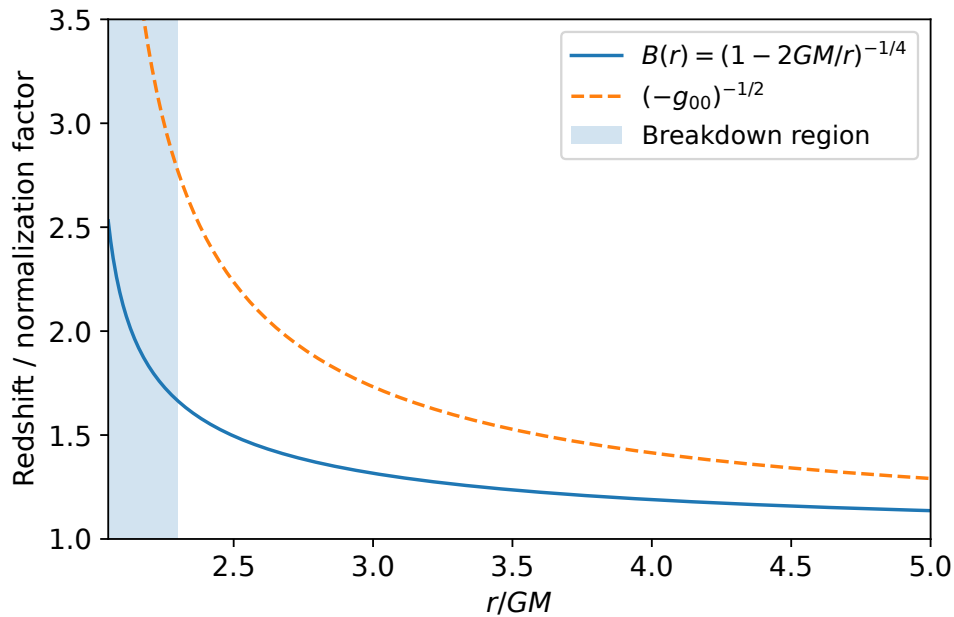


Figure 2. Comparison of the local amplitude normalization $B(r) = (1 - 2GM/r)^{-1/4}$ and the Tolman redshift factor $(-g_{00})^{-1/2} = (1 - 2GM/r)^{-1/2}$ in the Schwarzschild geometry. The factor $B(r)$ governs the local normalization of field amplitudes for static observers, while the Tolman factor describes the gravitational redshift of locally measured energy scales and temperature. Both diverge as $r \rightarrow 2GM$ for static coordinates, reflecting the infinite redshift of that frame rather than any enhancement of conserved flux at infinity. The shaded band marks a representative near-horizon region where the WKB and Riemann-normal expansions cease to be reliable. The precise location of this breakdown depends on the mode frequency: higher-frequency quanta remain within the domain of validity closer to the horizon, whereas modes with wavelengths comparable to the curvature scale satisfy $\varepsilon \gtrsim 0.3$ [see Equation (16)].

When these locality and hierarchy conditions are fulfilled, the LMC construction provides a reliable and computationally efficient framework for calculating curvature-sensitive amplitudes in weakly curved backgrounds while remaining consistent with standard semiclassical physics.

4. Curvature-Modified Feynman Rules and Example

Within the LMC framework, the standard Feynman-diagram expansion retains its topological structure, while curvature effects appear through multiplicative factors derived from the normalization function $B(x)$ and the gravitational phase $S(x)$. For scalar and spinor fields, we write

$$\Phi(x) = B(x) e^{iS(x)/\hbar} \phi_{\text{flat}}(\xi(x)), \quad \Psi(x) = B(x) e^{iS(x)/\hbar} \psi_{\text{flat}}(\xi(x)), \quad (18)$$

where ϕ_{flat} and ψ_{flat} are ordinary flat-space fields expressed in Riemann normal coordinates. The corresponding scalar propagator in a convex normal neighborhood is taken in Hadamard form,

$$G_F(x, x') = \frac{i}{8\pi^2} \left[\frac{U(x, x')}{\sigma(x, x') + i\epsilon} + V(x, x') \ln(\mu^2[\sigma(x, x') + i\epsilon]) + W(x, x') \right], \quad (19)$$

with $U(x, x') = \Delta^{1/2}(x, x')$ the Van Vleck–Morette biscalar and (V, W) smooth. *No single-point normalization factors $B(\cdot)$ appear in G_F ; all observer-dependent normalizations are assigned to external legs, as discussed below under External legs and observer frames.* Here $\Delta^{1/2}(x, x')$ carries the bi-local geodesic focusing. It is not duplicated by the single-point transport factors $B(x), B(x')$. Equation (19) is valid only inside convex normal neighborhoods, where $S(x)$ remains single-valued and $\xi(x)$ and $\xi(x')$ are connected by a unique geodesic. The multiplicative factors $B_u(x)$ and $S(x)$ act as a local dressing of propagators and external lines, while the diagram topology and combinatorics remain unchanged.

For a Yukawa interaction, we use the usual curved-space vertex density with invariant measure,

$$\mathcal{L}_{\text{int}}(x) = \lambda \bar{\Psi}(x) \Phi(x) \Psi(x), \quad \int d^4x \sqrt{-g(x)} \mathcal{L}_{\text{int}}(x). \quad (20)$$

Vertices carry no additional B factors; the invariant measure $\sqrt{-g} d^4x$ and the bi-local structure of G_F already encode the geometric effects. Observer-dependent normalizations B_u appear only on *external* legs, as discussed below.

All vertex integrals are evaluated with the curved-space measure $\sqrt{-g(x)} d^4x$, or equivalently $|\partial\bar{\zeta}/\partial x| d^4\bar{\zeta}$ in local coordinates. When stationary-phase approximations are used to match adjacent patches, the corresponding Jacobian factors ensure that the overall normalization of amplitudes remains covariant. In a stationary-phase evaluation of the vertex integrals, $\partial_{\bar{\zeta}}[S(x) - S(x')] = 0$ selects the geodesic saddle. The resulting Hessian determinant combines with $|\partial\bar{\zeta}/\partial x|$ to yield the Van Vleck determinant $\Delta^{1/2}(x, x')$, ensuring a unitary leading-order matching between patches.

Having established these ingredients, the curvature-dressed version of flat-space perturbation theory can be summarized by the following modified Feynman (LMC) rules:

1. Internal propagators: Use the Hadamard form (19) with $U = \Delta^{1/2}$. Do *not* attach any single-point B factors to G_F .
2. Vertices: Integrate with the invariant measure $\int d^4x \sqrt{-g} \mathcal{L}_{\text{int}}(x)$; no extra B factors at vertices.
3. External legs (observer-dependent): If amplitudes are defined with respect to an observer congruence u^μ , attach

$$\phi_{\text{ext}}(x) \longrightarrow B_u(x) \phi_{\text{ext}}(x), \quad B_u(x) = \left(\frac{\omega_{\text{loc}}(x)}{\omega_\infty} \right)^{-1/2}, \quad \omega_{\text{loc}}(x) \equiv -u^\mu k_\mu.$$

For static observers, $B_u(x) = (-g_{00})^{-1/4}$.

4. Patching/caustics: When multiple geodesics connect x and x' , sum saddle contributions, each with its own $\Delta^{1/2}$, and include the Maslov phase $e^{-i\pi\mu/2}$ per conjugate point.

Earlier heuristic formulae that multiplied propagators by $B(x)B(x')$ double-count the transport amplitude already contained in $U = \Delta^{1/2}$. In this final convention, B_u appears only on external legs. These rules retain the flat-space diagrammatic structure while incorporating gravitational redshift and phase effects. They enable local, curvature-sensitive amplitude calculations without requiring global mode expansions or a preferred vacuum state. We now clarify the observer-dependent normalization factor that appears on external legs.

External legs, observer frames, and the B_u factor

Let $u^\mu(x)$ be a timelike unit vector field (observer congruence) with local tetrad e_a^μ . Mode amplitudes normalized with respect to observer proper time τ scale as $(2\omega_{\text{loc}})^{-1/2}$ with $\omega_{\text{loc}}(x) \equiv -u^\mu k_\mu(x)$. If asymptotic particle definitions use a Killing time t (where it exists), then $\omega_\infty \equiv -\bar{\zeta}^\mu k_\mu$ and, in static regions, $\omega_{\text{loc}} = \omega_\infty / \sqrt{-\bar{\zeta}^2(x)}$ (Tolman relation). Thus

$$B_u(x) \equiv \left(\frac{\omega_{\text{loc}}(x)}{\omega_\infty} \right)^{-1/2}, \quad \text{so that} \quad B_{\text{static}}(x) = (-g_{00}(x))^{-1/4}. \quad (21)$$

B_u is *observer dependent* and therefore does not belong to covariant bi-local objects like $G_F(x, x')$. We assign B_u solely to external legs and local measurements.

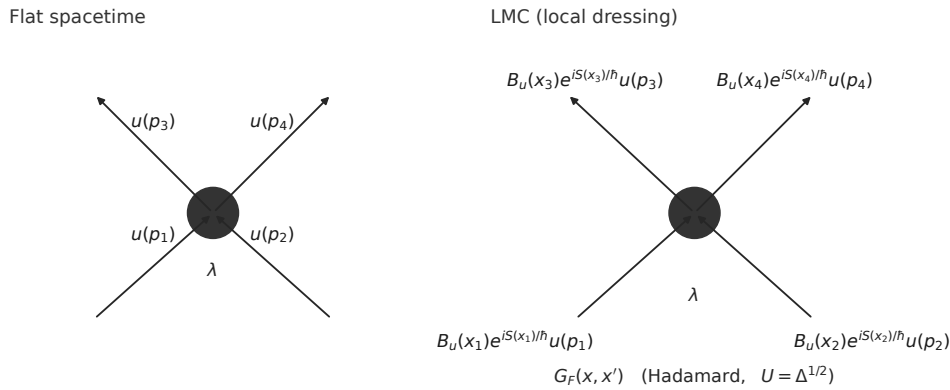


Figure 3. Comparison of a standard flat-spacetime Yukawa scattering diagram (left) with its locally dressed counterpart in the LMC formalism (right). Each external fermion line carries the observer-dependent normalization and phase factor $B_u(x_i)e^{iS(x_i)/\hbar}$. Internal propagators use the standard Hadamard form [Equation (19)], with $U(x, x') = \Delta^{1/2}(x, x')$. Vertices are integrated with the invariant measure $\sqrt{-g}d^4x$. Curvature enters exclusively through external-leg factors and local phases.

To illustrate the formalism, consider tree-level fermion–fermion scattering via scalar exchange in a weakly curved background. The corresponding diagrams are shown in Figure 3. The left panel represents the standard tree-level Yukawa vertex in flat spacetime, while the right panel illustrates the same process in the LMC framework. In the LMC framework, curvature dependence enters amplitudes through observer-dependent external-leg normalization factors and local phase accumulation, while internal propagators retain their standard curved-spacetime Hadamard form. Vertices are integrated with the invariant measure $\sqrt{-g}d^4x$ and do not carry additional single-point normalization factors. This separation avoids double counting of transport effects already encoded in the Van Vleck–Morette determinant and ensures consistency with covariant flux conservation.

These curvature-dependent terms encode redshift and phase effects locally but do not change the topology of the Feynman diagram. In flat spacetime, the amplitude is

$$\mathcal{M}_{\text{flat}} = -i\lambda^2 \bar{u}(p_3)u(p_1) \frac{1}{(p_1 + p_2)^2 - m^2 + i\epsilon} \bar{u}(p_4)u(p_2). \quad (22)$$

In the LMC framework, each external line and internal propagator is dressed according to Equations (18) and (19), giving

$$\mathcal{M}_{\text{LMC}} = -i\lambda^2 \prod_{i=1}^4 B_u(x_i) e^{i\int_{\Sigma_i} S(x_i)} \mathcal{M}_{\text{flat}}, \quad (23)$$

where x_i denote the external interaction points and (x, x') the endpoints of the internal scalar line. This expression incorporates curvature through the local normalization and phase functions while leaving the internal propagator in its standard curved-spacetime Hadamard form. The curvature dependence in Equation (23) enters only through the external-leg factors B_u and the local phases $S(x_i)$. Internal propagators retain the standard Hadamard form.

The curvature dependence in Equation (23) affects local amplitudes but cancels out of globally conserved quantities once proper redshift factors are included. The formalism therefore modifies the local representation of Feynman diagrams without changing their global observables, ensuring consistency with semiclassical energy conservation.

5. Applications and Phenomenology

We now apply the LMC formalism to describe local pair creation in the vicinity of a Schwarzschild horizon. This analysis parallels the standard Hawking process but is formulated entirely in terms of locally defined amplitudes. The Schwarzschild metric,

$$ds^2 = -\left(1 - \frac{2GM}{r}\right) dt^2 + \left(1 - \frac{2GM}{r}\right)^{-1} dr^2 + r^2 d\Omega^2, \quad (24)$$

admits a local inertial frame near any point $r_0 > 2GM$. From Equation (11), the normalization function becomes

$$B(r) = \left(1 - \frac{2GM}{r}\right)^{-1/4}, \quad (25)$$

which diverges formally as $r \rightarrow 2GM$. This divergence reflects the infinite redshift of static coordinates and marks the limit of validity of the local approximation rather than a physical divergence.

Schematic pair-creation amplitudes then take the form of local integrals of Hadamard two-point functions along with external-leg normalizations B_u appropriate to the chosen observer congruence.

Local Flux and Consistency with the Unruh State

The LMC assignment of local normalization and phase factors is arranged so that, when the global two-point function corresponds to the Unruh state, the standard point-splitting calculation reproduces the usual Hawking flux at \mathcal{I}^+ .

We sketch a stress-tensor check consistent with the Unruh vacuum. Using point-splitting with Hadamard subtraction, the renormalized flux component at future null infinity is

$$\langle T_{uu} \rangle_{\text{ren}} = \lim_{x' \rightarrow x} \mathcal{D}_{uu} [G_F(x, x') - G_H(x, x')], \quad (26)$$

where u is an affine retarded null coordinate, G_F is the exact two-point function in the Unruh state, G_H the local Hadamard parametrix with $U = \Delta^{1/2}$, and \mathcal{D}_{uu} the standard bi-differential operator for T_{uu} . In the near-horizon region, modes normalized with respect to static observers pick up the Tolman factor in their *external-leg* normalization, $B_{\text{static}} = (-g_{00})^{-1/4}$, while the *bi-local* singular structure is fixed entirely by $U = \Delta^{1/2}$ in (19). Propagating to \mathcal{S}^+ , the redshift of frequency $\omega_{\text{loc}} = \omega_{\infty} / \sqrt{-g_{00}}$ is exactly compensated by the external-leg normalization B_{static} , so the renormalized flux at infinity retains the Unruh value,

$$\langle T_{uu} \rangle_{\mathcal{S}^+} = \frac{\pi}{12} T_H^2 \quad (\text{per scalar d.o.f.}), \quad (27)$$

with $T_H = \kappa / (2\pi)$. This result follows from the standard relation $\langle T_{uu} \rangle_{\mathcal{S}^+} = (\pi/12) T_H^2$ for the Unruh vacuum, confirming that the LMC normalization assignment does not alter the conserved flux once redshift and proper-time normalization are accounted for. Greybody factors are encoded by the global radial wave operator and remain unchanged by our bookkeeping (since internal lines use the standard G_F in Hadamard form). This establishes that the LMC assignment— B_u on external legs only, with G_F bi-locally Hadamard—is consistent with the Hawking flux in the Unruh state.

The factors $B^n(x)$ represent only the redshift normalization of local amplitudes. When the radiation is propagated to asymptotic infinity, the redshift of energy exactly compensates for the local amplitude scaling, leaving the overall Hawking flux unchanged. The LMC framework therefore reproduces the standard Hawking result while providing a transparent local interpretation of the underlying processes.

The curvature-dependent normalization function $B(x)$ influences how field amplitudes are expressed in curved backgrounds but does not alter the total emission rate observed at infinity. In this sense, the LMC formalism provides a refined local description rather than a modification of Hawking's global result. It should be emphasized that the LMC construction itself does not determine the quantum state; the agreement with the Hawking flux follows only when the Unruh state is adopted as the global boundary condition.

Close to the horizon, the breakdown of the WKB expansion (where $g_{00} \rightarrow 0$) sets a natural cutoff for the applicability of Equation (25). Within its range of validity, the formalism describes a spatial redistribution of local field amplitudes that, in principle, may be probed in analogue-gravity experiments. Systems such as Bose–Einstein condensates and optical waveguides, where effective

horizons can be engineered, may provide accessible laboratory platforms to study curvature-modulated amplitude profiles and interference effects, as discussed in analogue-gravity systems [7].

Although the LMC factors $B(x)$ and $S(x)$ can be used to parameterize the spectrum locally, any interpretation of an “effective temperature” must be viewed as phenomenological rather than fundamental. The true Hawking temperature remains $T_H = 1/(8\pi GM)$, determined by the surface gravity of the black hole.

Overall, the LMC framework supplies a conceptually clear and computationally efficient way to treat quantum processes in weakly curved spacetimes while maintaining consistency with the established semiclassical picture of black-hole radiation.

6. Relation to Existing Frameworks

Several recent studies have explored local formulations of quantum field theory in curved spacetime that share conceptual similarities with the LMC approach. Li [5] proposed a WKB-based expansion in Riemann normal coordinates to study scalar and spinor propagation in weak gravitational fields, while MacKay [6] analyzed the consistency of this construction and identified the range where the weak-field approximation remains reliable.

The present work extends these ideas into a complete diagrammatic framework that integrates curvature effects directly into the building blocks of perturbative quantum field theory. Unlike earlier qualitative analyses, the LMC formulation provides explicit Feynman rules in which curvature enters through the observer-dependent factors $B_u(x)$ and the geometric phase $S(x)$, both derived from covariant current conservation and the Hamilton—Jacobi equation, ensuring internal consistency with the semiclassical limit.

In the limit of weak curvature, the LMC construction reproduces the standard results of QFT-CS while offering a transparent geometric interpretation of local propagation. For massless fields, $B(x)$ varies according to the congruence expansion, while curvature dependence enters primarily through the phase $S(x)$.

This work also clarifies the breakdown conditions emphasized by MacKay, showing that the WKB and Riemann-normal expansions become unreliable only very near the horizon ($r - 2GM \lesssim L_R$). Within the permitted domain, the formalism remains consistent with the Hawking result and standard energy conservation. Possible extensions include incorporating spin connections for fermions and treating gauge and tensor fields in a similar local manner. It is instructive to compare the LMC formalism with several well-known approaches to quantum field theory in curved spacetime.

We begin with the DeWitt–Schwinger method [8–10], which constructs the effective action and Green’s functions through a covariant short-distance expansion characterized by the Seeley–DeWitt coefficients. While this formalism excels in computing one-loop effects and trace anomalies, it is intrinsically nonlocal. In contrast, the LMC approach operates directly at the amplitude level, embedding curvature effects through the single-point factors $B_u(x)$ on external legs and the geometric phase $S(x)$, while the internal propagators remain the standard Hadamard bisolutions.

The Hadamard condition and algebraic QFT framework (e.g., [11–13]) provide a mathematically rigorous foundation for quantized fields in curved backgrounds. Although the LMC formalism is not expressed in this algebraic language, it is fully compatible with the principle of local covariance. The WKB-derived structures $B(x)$ and $S(x)$ reproduce the leading Hadamard singularity of two-point functions, ensuring physical consistency with the short-distance behavior prescribed by the Hadamard expansion.

In the LMC construction the inclusion of the Van Vleck determinant, as discussed in Sec. 3, guarantees that the two-point function possesses the correct Hadamard singularity. To leading order we have

$$G_F^{\text{LMC}}(x, x') = \frac{\Delta^{1/2}(x, x') e^{i[S(x) - S(x')]/\hbar}}{4\pi^2(\sigma + i\epsilon)} + O(\sigma^0), \quad (28)$$

which coincides with the standard parametrization of Hadamard states. As already evident from the local propagator in Equation (28), the factor $\Delta^{1/2}(x, x')$ ensures that the short-distance structure matches the Hadamard form given in Equation (19).

In the broader context of semiclassical gravity, the effective field theory (EFT) approach [14,15] treats general relativity as a low-energy expansion, organizing quantum corrections in powers of curvature and energy scale. The LMC framework is complementary as it captures the same curvature dependence directly at the level of local amplitudes rather than in the Lagrangian. In this way, the LMC construction bridges semiclassical propagation and perturbative QFT techniques while remaining agnostic about ultraviolet completion. Taken together, these comparisons show that the LMC method offers a conceptually clear and computationally efficient way to describe quantum processes in weakly curved backgrounds, connecting global QFT-CS results with local observer formulations.

7. Conclusions and Outlook

The LMC framework provides a concrete way to embed gravitational effects into perturbative quantum field theory. By introducing a curvature-dependent normalization function $B(x)$ and a gravitational phase $S(x)$ derived from covariant current conservation and WKB methods, the formalism extends flat-space Feynman diagrammatics to curved spacetimes while maintaining consistency with the equivalence principle.

A principal outcome of the LMC framework is that local curvature modifies the normalization of quantum field amplitudes according to $B(x) \propto (-g_{00})^{-1/4}$ in static metrics, while the gravitational phase $S(x)$ encodes redshift and geodesic propagation. When applied near a Schwarzschild horizon, these factors lead to a local modulation of field amplitudes but leave the total Hawking flux and temperature unchanged once redshift to infinity is included. Because the construction is local by design, it is well suited for applications where global mode decompositions are impractical, including dynamically evolving backgrounds and analogue-gravity settings. Laboratory systems such as Bose-Einstein condensates and optical waveguides may provide platforms to explore curvature-dependent amplitude modulation and interference effects within such local descriptions.

Future work will extend the LMC formulation to include spin connections for fermions, gauge fields, and linearized gravitational perturbations. Loop corrections and renormalization-group effects can be organized naturally around the curvature-sensitive factors $B_u(x)$ and $S(x)$, offering a new perspective on semiclassical processes in curved spacetime. Loop integrals can be evaluated patchwise using the same local measure $\sqrt{-g} d^4x$, with curvature entering through the Van Vleck determinant $\Delta^{1/2}$ and the associated Jacobian factors. These developments will further clarify the connection between local field dynamics and the global properties of spacetime geometry.

A brief discussion of spinor and gauge-field extensions of the formalism is provided in the Appendix.

The present treatment is confined to leading WKB order within convex normal neighborhoods. Global vacuum selection, greybody transmission, and higher-order transport corrections lie beyond the local construction. Extending the LMC formalism to one-loop order and explicitly matching to the DeWitt–Schwinger coefficients would be valuable future work.

Appendix A. Spinor and Gauge-Field Extensions

The LMC formalism extends naturally to spinor and gauge fields once the spin connection and local tetrad structure are introduced. In curved spacetime, the covariant derivative acting on a spinor field is

$$D_\mu \Psi = \partial_\mu \Psi + \frac{1}{4} \omega_{ab\mu} \gamma^{[a} \gamma^{b]} \Psi, \quad (\text{A1})$$

where $\omega_{ab\mu}$ is the spin connection built from the tetrad e^a_μ satisfying $g_{\mu\nu} = e^a_\mu e^b_\nu \eta_{ab}$ [10,11].

To leading order in weak curvature, the LMC ansatz $\Psi(x) \simeq B_\psi(x) e^{iS(x)/\hbar} \psi_{\text{flat}}(\xi)$ remains valid, with $B_\psi(x)$ determined by the covariant current conservation law, Equation (8). The spin connection contributes only subleading corrections to $S(x)$ in the WKB hierarchy. For gauge fields, the same

construction applies in Lorenz gauge $\nabla_\mu A^\mu = 0$, where curvature enters through the normalization $B_A(x)$ and the gravitational phase $S(x)$ that governs the transport of polarization vectors along geodesics. These extensions show that the LMC prescription extends straightforwardly to all field spins in the semiclassical regime.

For $ds^2 = -f(r)dt^2 + f^{-1}(r)dr^2 + r^2d\Omega^2$, the WKB ansatz $\Psi = B_\psi e^{iS/\hbar} u$ gives, at leading orders,

$$(\gamma^a e_a^\mu \partial_\mu S - m)u = 0, \quad (\text{A2})$$

$$2\partial_\mu S \nabla^\mu B_\psi + B_\psi \square S = 0, \quad (\text{A3})$$

where ∇_μ includes the spin connection $\omega_{\mu ab}$. Current conservation $\nabla_\mu(\bar{\Psi}\gamma^\mu\Psi) = 0$ then yields $B_\psi \propto (-g_{00})^{-1/4}$, consistent with the scalar result and confirming that the spin connection affects only subleading phase corrections in $S(x)$.

References

- Hawking, S.W. Particle Creation by Black Holes. *Communications in Mathematical Physics* **1975**, *43*, 199–220. <https://doi.org/10.1007/BF02345020>.
- Parker, L. Quantized Fields and Particle Creation in Expanding Universes. I. *Phys. Rev.* **1969**, *183*, 1057–1068. <https://doi.org/10.1103/PhysRev.183.1057>.
- Parker, L. Quantized Fields and Particle Creation in Expanding Universes. II. *Phys. Rev. D* **1971**, *3*, 346–356. <https://doi.org/10.1103/PhysRevD.3.346>.
- Unruh, W.G. Notes on black-hole evaporation. *Physical Review D* **1976**, *14*, 870–892. <https://doi.org/10.1103/PhysRevD.14.870>.
- Li, B. The Modification of Feynman Diagrams in Curved Space-Time. *arXiv:2411.15164* **2024**.
- MacKay, N.M. Remarks on "The Modification of Feynman Diagrams in Curved Space-Time". *arXiv:2501.15672* **2025**.
- Visser, M. Acoustic black holes: Horizons, ergospheres, and Hawking radiation. *Classical and Quantum Gravity* **1998**, *15*, 1767–1791. <https://doi.org/10.1088/0264-9381/15/6/024>.
- DeWitt, B.S. Quantum Field Theory in Curved Spacetime. *Physics Reports* **1975**, *19*, 295–357. [https://doi.org/10.1016/0370-1573\(75\)90051-4](https://doi.org/10.1016/0370-1573(75)90051-4).
- Birrell, N.D.; Davies, P.C.W. *Quantum Fields in Curved Space*; Cambridge Monographs on Mathematical Physics, Cambridge University Press, 1982.
- Parker, L.; Toms, D. *Quantum Field Theory in Curved Spacetime: Quantized Fields and Gravity*; Cambridge Monographs on Mathematical Physics, Cambridge University Press, 2009.
- Wald, R.M. *Quantum Field Theory in Curved Spacetime and Black Hole Thermodynamics*; University of Chicago Press, 1994.
- Brunetti, R.; Fredenhagen, K. Microlocal Analysis and Interacting Quantum Field Theories: Renormalization on Physical Backgrounds. *Communications in Mathematical Physics* **2000**, *208*, 623–661. <https://doi.org/10.1007/s002200050004>.
- Hollands, S.; Wald, R.M. Local Wick Polynomials and Time Ordered Products of Quantum Fields in Curved Spacetime. *Communications in Mathematical Physics* **2001**, *223*, 289–326. <https://doi.org/10.1007/s002200100540>.
- Donoghue, J.F. General Relativity as an Effective Field Theory: The Leading Quantum Corrections. *Physical Review D* **1994**, *50*, 3874–3888. <https://doi.org/10.1103/PhysRevD.50.3874>.
- Burgess, C.P. Quantum gravity in everyday life: General relativity as an effective field theory. *Living Reviews in Relativity* **2004**, *7*, 5. <https://doi.org/10.12942/lrr-2004-5>.

Disclaimer/Publisher's Note: The statements, opinions and data contained in all publications are solely those of the individual author(s) and contributor(s) and not of MDPI and/or the editor(s). MDPI and/or the editor(s) disclaim responsibility for any injury to people or property resulting from any ideas, methods, instructions or products referred to in the content.